J. Fluid Mech. (1985), *vol.* 152, *pp.* 1–13
Printed in Great Britain

A model for Stokes flow in a two-dimensional bifurcating channel

By K. B. RANGER
Department of Mathematics, University of Toronto, Canada M5S 1A1
AND H. BRENNER
Department of Chemical Engineering, Massachusetts Institute of Technology, Cambridge, Massachusetts, U.S.A.

(Received 1 July 1983 and in revised form 27 August 1984)

A model is presented for steady two-dimensional Stokes flow in a bifurcating channel. The geometry of the bifurcation is symmetric, but the flow rates through the two branches may be unequal. It is found that separation takes place on the outer boundary of the channel for either a smooth or a sharp flow divider, but only when the flow rates through the two branches of the channel are sufficiently different.

1. Introduction

The motion of a viscous fluid through a bifurcating channel is of interest in physiology and engineering science. A mathematical description of the general problem presents difficulties due to the complexities of the boundary geometry which is fully three-dimensional. In addition, the flows of interest take place at large Reynolds number, and the motion may be pulsatile. It is because of these facts that most of the useful information concerning bifurcating flows has been determined empirically (see Pedley 1980).

There is a scarcity of solutions to boundary-value problems in fluid mechanics that contain a flow divider, even in potential flow and also at low Reynolds numbers. This is the motivation for the present work.

In this paper a two-dimensional Stokes-flow model of a bifurcation is presented for the motion inside a cylinder whose cross-section is an elliptic limaçon. For certain values of the parameter describing the limaçon, the boundary has a convex indentation which becomes a cusp in the limiting case of a cardioid. This indentation plays the role of a flow divider, and the motion is caused by a line source at the point where the positive axis meets the boundary curve and is absorbed away by two line sinks, in general of unequal strengths, located at points in the two branches of the channel.

It is possible to determine a two-dimensional harmonic function satisfying the boundary conditions, explicitly, and in a finite form. The main interest centres on the shear stress at the boundary, or equivalently the boundary vorticity. Owing to the fact that there is a spreading on the coefficients contained in the stream function ψ (that is, the arbitrary coefficients in ψ are determined by difference and not simultaneous equations) it follows that the boundary vorticity is found in a finite but cumbersome form. It is found that when the flow divider is present the boundary vorticity may change on the boundary of weaker sink strength, thus indicating a region of reversed flow attached to the wall. Separation has been observed experimentally in three-dimensional flow by Schroter & Sudlow (1969) and by Smith, Cotton & Freedman (1974) for a two-dimensional bifurcation. Some numerical values are given for the vorticity on the boundary for different values of the parameter describing the boundary geometry and also for various distances along the boundary. It is worth mentioning that when separation takes place in Stokes flow it is almost certain to occur at higher Reynolds numbers, even though the separation region is modified. Another point is that there is a strong analogy between two- and three-dimensional Stokes flow for flows in which separation takes place. This has been demonstrated by Dorrepaal (1979) for the case of flow past a circular arc and by Dorrepaal, O'Neill & Ranger (1976) for the streaming flow past a spherical cap.

The presence of separation in the model considered in this paper can be attributed to the presence of the flow divider, since in the corresponding flow inside a circle there is no separation regardless of the relative strengths of the sinks (see Ranger 1961).

2. Geometry of bifurcation

Consider the conformal transformation

$$z = x+\mathrm{i}y = (1+\epsilon\zeta)^2, \quad 0 < \epsilon \leqslant 1, \tag{1}$$

where $\zeta = \xi+\mathrm{i}\eta = \rho\,\mathrm{e}^{\mathrm{i}\phi}$. The real and imaginary parts of z are

$$x = 1+2\epsilon\rho\cos\phi+\epsilon^2\rho^2\cos 2\phi, \tag{2}$$

$$y = 2\epsilon\rho\sin\phi+\epsilon^2\rho^2\sin 2\phi. \tag{3}$$

The interior of the unit circle $0 \leqslant \rho \leqslant 1$ in the ζ-plane is mapped conformally into the interior of an elliptic limaçon in the z-plane. For $0 < \epsilon < \frac{1}{2}$ the boundary is everywhere concave to the interior region, but for $\frac{1}{2} < \epsilon \leqslant 1$ the boundary has a convex indentation with nose at $\rho = 1$, $\phi = \pi$; see figures 1–3. The indentation becomes a cusp at $\epsilon = 1$, which corresponds to the case of a cardioid, the origin being the sharp point of the cusp. In the case of the cardioid the boundary ranges from $-\frac{1}{2} < x \leqslant 4$ and $|y| \leqslant \frac{3}{2}\sqrt{3}$. The maximum value of y occurs at $\phi = \frac{1}{3}\pi$. The least value of x occurs at $\phi = \frac{2}{3}\pi$, and the largest at $\phi = 0$. Also, in the case $\epsilon = 1$ the point $\rho = 1$, $\phi = \pi$ is a point of transformation (1) which is not conformal.

The convex indentation plays the role of a flow divider in a model of viscous flow through a two-dimensional bifurcating channel. The motion is created by a line source at $\rho = 1$, $\phi = 0$ and is absorbed away by two line sinks (in general of unequal strengths) located at $\rho = 1$, $\phi = \pm\alpha$, $\frac{1}{2}\pi < \alpha < \pi$. In the case of the cardioid, α can be taken as $\frac{2}{3}\pi$, which corresponds to the point most remote from the origin, parallel to the x-axis.

3. Equations of motion and method of solution

For steady two-dimensional flow the fluid velocity can be prescribed in terms of an Earnshaw stream function ψ by

$$\boldsymbol{q} = \operatorname{curl}\{-\psi\boldsymbol{k}\}, \tag{4}$$

where $\boldsymbol{k}$ is the unit vector perpendicular to the plane of motion. In the absence of convection terms the Stokes equations are, in non-dimensional form,

$$\frac{\partial p}{\partial x} = -\frac{\partial}{\partial y}\nabla_1^2\psi, \quad \frac{\partial p}{\partial y} = \frac{\partial}{\partial x}\nabla_1^2\psi, \tag{5}$$

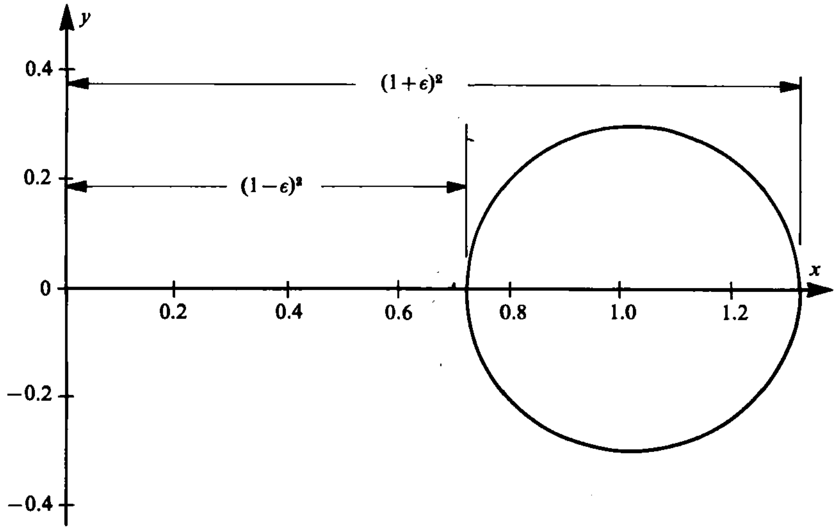

FIGURE 1. $0 < \epsilon < \frac{1}{2}$; no indentation (the explicit plot shown is for $\epsilon = 0.15$).

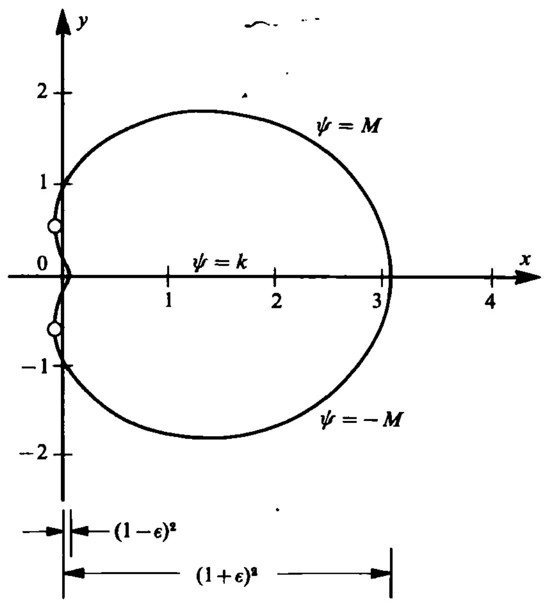

FIGURE 2. $\frac{1}{2} < \epsilon < 1$; smooth flow divider (the explicit plot shown is for $\epsilon = 0.75$).

where p is the pressure and $\nabla_1^2 \equiv \partial^2/\partial x^2 + \partial^2/\partial y^2$ is the two-dimensional Laplacian. If the pressure is eliminated from (5) the stream function satisfies the biharmonic equation

$$\nabla_1^4 \psi = 0. \tag{6}$$

A suitable representation for ψ in the present case is

$$\psi = \psi_1 + x\psi_2, \tag{7}$$

where ψ_1 and ψ_2 are two-dimensional harmonics satisfying

$$\nabla_1^2 \psi_1 = 0, \quad \nabla_1^2 \psi_2 = 0. \tag{8}$$

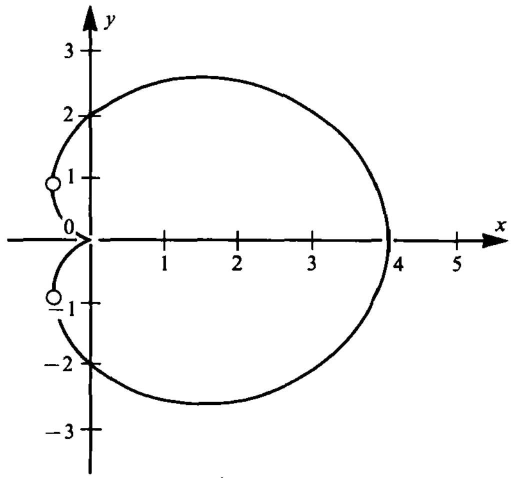

FIGURE 3. $\epsilon = 1$; cardioid flow divider has a cusp at the origin.

It follows from (5) and (7) that the pressure can be related to ψ_2 in the form

$$p = -2\frac{\partial \psi_2}{\partial y}. \tag{9}$$

Since the two-dimensional Laplace equation is conformally invariant under the transformation (1), appropriate general forms in (ρ, ϕ)-coordinates for ψ_1 and ψ_2 are

$$\psi_1 = \sum_{n=1}^{\infty} A_n \rho^n \sin n\phi + \sum_{n=0}^{\infty} c_n \rho^n \cos n\phi, \tag{10}$$

$$\psi_2 = \sum_{n=1}^{\infty} B_n \rho^n \sin n\phi + \sum_{n=0}^{\infty} D_n \rho^n \cos n\phi, \tag{11}$$

where the coefficients A_n, B_n, C_n, D_n are to be determined. If (10) and (11) are substituted in (7), then ψ may be expressed by

$$\begin{aligned}
\psi = {} & \{(A_1+B_1)\rho + B_2\rho^3\epsilon + \tfrac{1}{2}\epsilon^2 B_3 \rho^5 - \tfrac{1}{2}\epsilon^2 B_1 \rho^3\} \sin\phi \\
& + \{(A_2+B_2)\rho^2 + B_1\rho^2\epsilon + B_3\rho^4\epsilon + \tfrac{1}{2}B_4\epsilon^2\rho^6\} \sin 2\phi \\
& + \sum_{n=3}^{\infty} \{(A_n+B_n)\rho^n + \epsilon B_{n-1}\rho^n + \epsilon\rho^{n+2}B_{n+1} + \tfrac{1}{2}\epsilon^2 B_{n-2}\rho^n + \tfrac{1}{2}\epsilon^2 B_{n+2}\rho^{n+4}\} \sin n\phi \\
& + C_0 + D_0 + \epsilon D_1 \rho^2 + \tfrac{1}{2}\epsilon^2 D_2 \rho^4 \\
& + [(C_1+D_1)\rho + \epsilon D_0\rho + \epsilon(D_0\rho + D_2\rho^3) + \tfrac{1}{2}\epsilon^2(D_1\rho^3 + D_3\rho^5)] \cos\phi \\
& + [(C_2+D_2)\rho^2 + \epsilon D_1\rho^2 + \epsilon D_3\rho^4 + \tfrac{1}{2}\epsilon^2 D_0\rho^2 + \tfrac{1}{2}\epsilon^2(D_0\rho^2 + D_4\rho^6)] \cos 2\phi \\
& + \sum_{n=3}^{\infty} [(C_n+D_n)\rho^n + \epsilon D_{n-1}\rho^n + \epsilon D_{n+1}\rho^{n+2} + \tfrac{1}{2}\epsilon^2 D_{n-2}\rho^n + \tfrac{1}{2}\epsilon^2 D_{n+2}\rho^{n+4}] \cos n\phi.
\end{aligned} \tag{12}$$

Taking account of the source and sinks, the appropriate boundary conditions are on $\rho = 1$

$$\left.\begin{aligned}
\psi &= M \ (0 < \phi < \alpha), & \psi &= k \ (\alpha < \phi < \pi), \\
\psi &= -M \ (0 > \phi > -\alpha), & \psi &= k \ (-\alpha > \phi > -\pi),
\end{aligned}\right\} \tag{13}$$

and

$$\frac{\partial \psi}{\partial \rho} = 0 \quad \text{at } \rho = 1 \quad (-\pi < \phi < \pi). \tag{14}$$

The symmetric case has $k = 0$: the ratio k/M is a measure of the asymmetry of the flows into the two sinks. For $n \geqslant 3$ the Fourier components of $\sin n\phi$ give

$$A_n + B_n + \epsilon B_{n-1} + \epsilon B_{n+1} + \tfrac{1}{2}\epsilon^2 B_{n-2} + \tfrac{1}{2}\epsilon^2 B_{n+2}$$
$$= \frac{1}{\pi}\int_{-\pi}^{\pi} \psi(1,\phi)\sin n\phi \,\mathrm{d}\phi = \frac{2M}{\pi}\int_0^{\alpha} \sin n\phi\,\mathrm{d}\phi$$
$$= \frac{2M}{\pi}\frac{1-\cos n\alpha}{n}, \tag{15}$$

and from (14)

$$nA_n + nB_n + n\epsilon B_{n-1} + \epsilon(n+2)B_{n+1} + \tfrac{1}{2}n\epsilon^2 B_{n-2} + \tfrac{1}{2}\epsilon^2 B_{n+2}(n+4) = 0. \tag{16}$$

Elimination of A_n yields

$$\epsilon B_{n+1} + \epsilon^2 B_{n+2} = \frac{M}{\pi}(\cos n\alpha - 1), \quad n \geqslant 3, \tag{17}$$

and the solution (see Appendix A) is given by

$$B_{n+2} = -\frac{M}{\pi\epsilon(1+\epsilon)} + \frac{M}{\pi\epsilon}\frac{\cos(n+1)\alpha}{1+2\epsilon\cos\alpha+\epsilon^2} + \frac{M}{\pi}\frac{\cos n\alpha}{1+2\epsilon\cos\alpha+\epsilon^2} \tag{18}$$

for $n \geqslant 3$. The coefficients B_n, $n = 1, \ldots, 4$ are also given in Appendix A. The series $\Sigma_{n=2}^{\infty} B_n \rho^n \sin n\phi$ can be summed by standard methods, and is given in Appendix A. Again, for $n \geqslant 3$ the Fourier component in $\cos n\phi$ gives

$$C_n + D_n + \epsilon D_{n-1} + \epsilon D_{n+1} + \tfrac{1}{2}\epsilon^2 D_{n-2} + \tfrac{1}{2}\epsilon^2 D_{n+2}$$
$$= \frac{1}{\pi}\int_{-\pi}^{\pi} \psi(1,\phi)\cos n\phi\,\mathrm{d}\phi = \frac{2k}{\pi}\int_{\alpha}^{\pi}\cos n\phi\,\mathrm{d}\phi = -\frac{2k\sin n\alpha}{\pi n} \tag{19}$$

and $$nC_n + nD_n + n\epsilon D_{n-1} + (n+2)\epsilon D_{n+1} + \tfrac{1}{2}\epsilon^2 n D_{n-2} + \tfrac{1}{2}\epsilon^2 D_{n+2}(n+4) = 0. \tag{20}$$

Elimination of C_n from (19) and (20) yields the following difference equation for the coefficients D_n:

$$\epsilon D_{n+1} + \epsilon^2 D_{n+2} = \frac{k\sin n\alpha}{\pi}, \quad n \geqslant 3. \tag{21}$$

The solution is described in Appendix B, and is given by

$$D_{n+2} = \frac{k\sin(n+1)\alpha + k\epsilon\sin n\alpha}{\pi\epsilon(1+2\epsilon\cos\alpha+\epsilon^2)}, \quad n \geqslant 3. \tag{22}$$

Equations are also given for D_1, D_2, D_3, D_4 in Appendix B. Also, from Appendix B, the series $\Sigma_{n=3}^{\infty} D_{n+2}\rho^{n+2}\cos(n+2)\phi$ can be summed by standard methods.

It follows that the harmonic function ψ_2 is uniquely determined, and is expressed by

$$\begin{aligned}
\psi_2 = {} & B_2\rho^2\sin 2\phi + B_3\rho^3\sin 3\phi + B_4\rho^4\sin 4\phi + D_1\rho\cos\phi + D_2\rho^2\cos 2\phi \\
& + D_3\rho^3\cos 3\phi + D_4\rho^4\cos 4\phi - \frac{M}{\pi\epsilon(1+\epsilon)}\left\{\frac{\rho^5\sin 5\phi - \rho^6\sin 4\phi}{1-2\rho\cos\phi+\rho^2}\right\} \\
& + \frac{M+k}{2\pi\epsilon}\left\{\frac{\rho^5\sin(5\phi+4\alpha) - \rho^6\sin(4\phi+3\alpha) + \epsilon\rho^5\sin(5\phi+3\alpha) - \epsilon\rho^6\sin(4\phi+2\alpha)}{(1+2\epsilon\cos\alpha+\epsilon^2)(1-2\rho\cos(\phi+\alpha)+\rho^2)}\right\} \\
& + \frac{M-k}{2\pi\epsilon}\left\{\frac{\rho^5\sin(5\phi-4\alpha) - \rho^6\sin(4\phi-3\alpha) + \epsilon\rho^5\sin(5\phi-3\alpha) - \epsilon\rho^6\sin(4\phi-2\alpha)}{(1+2\epsilon\cos\alpha+\epsilon^2)(1-2\rho\cos(\phi-\alpha)+\rho^2)}\right\}.
\end{aligned} \tag{23}$$

The vorticity ω in (ρ,ϕ)-coordinates is given by

$$\omega = \frac{1}{4\epsilon^2(1+2\epsilon\rho\cos\phi+\epsilon^2\rho^2)}\left\{(\epsilon\cos\phi+\epsilon^2\rho\cos 2\phi)\frac{\partial\psi_2}{\partial\rho}-\frac{\epsilon\sin\phi+\epsilon^2\rho\sin 2\phi}{\rho}\frac{\partial\psi_2}{\partial\phi}\right\}, \quad (24)$$

and on the boundary $\rho = 1$

$$\omega = \frac{1}{4\epsilon^2(1+2\epsilon\cos\phi+\epsilon^2)}\left\{(\epsilon\cos\phi+\epsilon^2\cos 2\phi)\left.\frac{\partial\psi_2}{\partial\rho}\right|_{\rho=1}-(\epsilon\sin\phi+\epsilon^2\sin 2\phi)\left.\frac{\partial\psi_2}{\partial\phi}\right|_{\rho=1}\right\} \quad (25)$$

$$= \frac{1}{4\epsilon^2}\frac{W}{(1+2\epsilon\cos\phi+\epsilon^2)}, \quad (26)$$

where W is defined by

$$\begin{aligned}W = {}& 2\epsilon B_2\sin\phi+3B_3(\epsilon\sin 2\phi+\epsilon^2\sin\phi)\\
&+4B_4(\epsilon\sin 3\phi+\epsilon^2\sin 2\phi)+\sum_{s=1}^{4} sD_s[\epsilon\cos(s-1)\phi+\epsilon^2\cos(s-2)\phi]\\
&+\frac{\epsilon\cos\phi+\epsilon^2\cos 2\phi}{\pi\epsilon}\left\{\frac{5\sin 4\phi-4\sin 5\phi}{(1+\epsilon)(1-\cos\phi)}\right.\\
&+\frac{M+k}{4}\left\{\frac{4\sin(5\phi+4\alpha)-5\sin(4\phi+3\alpha)+4\epsilon\sin(5\phi+3\alpha)-5\epsilon\sin(4\phi+2\alpha)}{(1+2\epsilon\cos\alpha+\epsilon^2)[1-\cos(\phi+\alpha)]}\right\}\\
&\left.+\frac{M-k}{4}\left\{\frac{4\sin(5\phi-4\alpha)-5\sin(4\phi-3\alpha)+4\epsilon\sin(5\phi-3\alpha)-5\epsilon\sin(4\phi-2\alpha)}{(1+2\epsilon\cos\alpha+\epsilon^2)[1-\cos(\phi-\alpha)]}\right\}\right\}\\
&-\frac{\epsilon\sin\phi+\epsilon^2\sin 2\phi}{\pi\epsilon}\left\{(1+\epsilon)\left[\frac{4\cos 4\phi-5\cos 5\phi}{1-\cos\phi}-\frac{(\sin 4\phi-\sin 5\phi)\sin\phi}{(1-\cos\phi)^2}\right]\right.\\
&+\frac{M+k}{4}\left\{\frac{5\cos(5\phi+4\alpha)-4\cos(4\phi+3\alpha)+5\epsilon\cos(5\phi+3\alpha)-4\epsilon\cos(4\phi+2\alpha)}{(1+2\epsilon\cos\alpha+\epsilon^2)(1-\cos(\phi+\alpha))}\right\}\\
&-\frac{M+k}{4}\left\{\frac{\sin(5\phi+4\alpha)-\sin(4\phi+3\alpha)+\epsilon\sin(5\phi+3\alpha)-\epsilon\sin(4\phi+2\alpha)}{(1+2\epsilon\cos\alpha+\epsilon^2)(1-\cos(\phi+\alpha))^2}\right\}\sin(\phi+\alpha)\\
&+\frac{M-k}{4}\left\{\frac{5\cos(5\phi-4\alpha)-4\cos(4\phi-3\alpha)+5\epsilon\cos(5\phi-3\alpha)-4\epsilon\cos(4\phi-2\alpha)}{(1+2\epsilon\cos\alpha+\epsilon^2)(1-\cos(\phi-\alpha))}\right\}\\
&-\frac{M-k}{4}\left\{\frac{\sin(5\phi-4\alpha)-\sin(4\phi-3\alpha)+\epsilon\sin(5\phi-3\alpha)-\epsilon\sin(4\phi-2\alpha)}{(1+2\epsilon\cos\alpha+\epsilon^2)[1-\cos(\phi-\alpha)]^2}\right\}\\
&\left.\times\sin(\phi-\alpha)\right\}. \end{aligned} \quad (27)$$

The most interesting feature of the flow is the calculation of the outer wall stress, or equivalently the vorticity on the boundary $\rho = 1$. To this end it suffices to determine the function ψ_2 which forms part of the stream function ψ. Also it is only necessary to calculate the boundary vorticity for various values of k/M and ϵ in the range $0 < \phi < \alpha$. As already explained, α can be taken as $\frac{2}{3}\pi$. The vorticity is locally large and negative at $\phi = 0+$ and $\phi = \frac{2}{3}\pi-$, where the effects of the line source and sink dominate the flow. Numerical values for the boundary vorticity are given in tables 1–3 and in figures 4–6, for the cases $\epsilon = 0.5$ where there is no flow divider, $\epsilon = 0.95$ where the flow divider is smooth, and $\epsilon = 1$ where the flow divider is a cusp. These values indicate that for sufficiently large values of k, $0 \leqslant k < M$, there is a

k/M \ ϕ	0.25	0.50	0.75	1.00	1.25	1.50	1.75	2.00
0.00	−5.38974	−2.78489	−1.97036	−1.62476	−1.50599	−1.58948	−2.08585	−5.85002
0.05	−5.35644	−2.75061	−1.93423	−1.58539	−1.46088	−1.53299	−2.00000	−5.57327
0.10	−5.32315	−2.71634	−1.89809	−1.54602	−1.41577	−1.47650	−1.91415	−5.29651
0.15	−5.28985	−2.68207	−1.86195	−1.50665	−1.37065	−1.42001	−1.82831	−5.01976
0.20	−5.25655	−2.64779	−1.82582	−1.46728	−1.32554	−1.36351	−1.74246	−4.74301
0.25	−5.22326	−2.61352	−1.78968	−1.42791	−1.28043	−1.30702	−1.65661	−4.46625
0.30	−5.18996	−2.57924	−1.75355	−1.38854	−1.23532	−1.25053	−1.57077	−4.18950
0.35	−5.15666	−2.54497	−1.71741	−1.34917	−1.19020	−1.19404	−1.48492	−3.91274
0.40	−5.12336	−2.51070	−1.68128	−1.30980	−1.14509	−1.13755	−1.39907	−3.63599
0.45	−5.09007	−2.47642	−1.64514	−1.27043	−1.09998	−1.08105	−1.31322	−3.35923
0.50	−5.05677	−2.44215	−1.60900	−1.23107	−1.05487	−1.02456	−1.22738	−3.08248
0.55	−5.02347	−2.40787	−1.57287	−1.19170	−1.00975	−0.96807	−1.14153	−2.80572
0.60	−4.99018	−2.37360	−1.53673	−1.15233	−0.96464	−0.91158	−1.05568	−2.52897
0.65	−4.95688	−2.33932	−1.50060	−1.11296	−0.91953	−0.85508	−0.96984	−2.25221
0.70	−4.92358	−2.30505	−1.46446	−1.07359	−0.87442	−0.79859	−0.88399	−1.97546
0.75	−4.89029	−2.27078	−1.42833	−1.03422	−0.82930	−0.74210	−0.79814	−1.69870
0.80	−4.85699	−2.23650	−1.39219	−0.99485	−0.78419	−0.68561	−0.71230	−1.42195
0.85	−4.82369	−2.20223	−1.35605	−0.95548	−0.73908	−0.62912	−0.62645	−1.14519
0.90	−4.79040	−2.16795	−1.31992	−0.91611	−0.69397	−0.57262	−0.54060	−0.86844
0.95	−4.75710	−2.13368	−1.28378	−0.87674	−0.64885	−0.51613	−0.45475	−0.59169
1.00	−4.72380	−2.09941	−1.24765	−0.83737	−0.60374	−0.45964	−0.36891	−0.31493

TABLE 1. Calculation of vorticity W as a function of ϕ for $\epsilon = 0.50$

k/M \ ϕ	0.25	0.50	0.75	1.00	1.25	1.50	1.75	2.00
0.00	−6.03971	−3.16424	−2.28998	−1.94709	−1.87381	−2.06426	−2.83638	−8.33290
0.05	−5.96125	−3.08436	−2.20740	−1.85983	−1.77823	−1.95219	−2.68178	−7.90171
0.10	−5.88279	−3.00449	−2.12482	−1.77256	−1.68264	−1.84012	−2.52718	−7.47052
0.15	−5.80433	−2.92461	−2.04225	−1.68530	−1.58706	−1.72806	−2.37258	−7.03933
0.20	−5.72586	−2.84473	−1.95967	−1.59804	−1.49148	−1.61599	−2.21798	−6.60814
0.25	−5.64740	−2.76485	−1.87710	−1.51078	−1.39590	−1.50392	−2.06339	−6.17695
0.30	−5.56894	−2.68497	−1.79452	−1.42352	−1.30032	−1.39185	−1.90879	−5.74576
0.35	−5.49048	−2.60509	−1.71195	−1.33626	−1.20474	−1.27978	−1.75419	−5.31457
0.40	−5.41201	−2.52522	−1.62937	−1.24900	−1.10916	−1.16772	−1.59959	−4.88339
0.45	−5.33355	−2.44534	−1.54680	−1.16174	−1.01358	−1.05565	−1.44499	−4.45220
0.50	−5.25509	−2.36546	−1.46422	−1.07448	−0.91800	−0.94358	−1.29040	−4.02101
0.55	−5.17663	−2.28558	−1.38165	−0.98722	−0.82242	−0.83151	−1.13580	−3.58982
0.60	−5.09816	−2.20570	−1.29907	−0.89996	−0.72683	−0.71944	−0.98120	−3.15863
0.65	−5.01970	−2.12583	−1.21650	−0.81270	−0.63125	−0.60737	−0.82660	−2.72744
0.70	−4.94124	−2.04595	−1.13392	−0.72544	−0.53567	−0.49531	−0.67200	−2.29625
0.75	−4.86278	−1.96607	−1.05135	−0.63818	−0.44009	−0.38324	−0.51740	−1.86506
0.80	−4.78431	−1.88619	−0.96877	−0.55092	−0.34451	−0.27217	−0.36281	−1.43388
0.85	−4.70585	−1.80631	−0.88619	−0.46366	−0.24893	−0.15910	−0.20821	−1.00269
0.90	−4.62739	−1.72643	−0.80362	−0.37639	−0.15335	−0.04703	−0.05361	−0.57150
0.95	−4.54893	−1.64656	−0.72104	−0.28913	−0.05777	0.06504	0.10099	−0.14031
1.00	−4.47046	−1.56668	−0.63847	−0.20187	0.03781	0.17710	0.25559	0.29088

TABLE 2. Calculation of vorticity W as a function of ϕ for $\epsilon = 0.95$

k/M \ ϕ	0.25	0.50	0.75	1.00	1.25	1.50	1.75	2.00
0.00	−6.09504	−3.19825	−2.32042	−1.97952	−1.91248	−2.11587	−2.91999	−8.61451
0.05	−6.00798	−3.10973	−2.22910	−1.88335	−1.80769	−1.99401	−2.75411	−8.16227
0.10	−5.92092	−3.02120	−2.13778	−1.78718	−1.70291	−1.87216	−2.58822	−7.71002
0.15	−5.83386	−2.93267	−2.04647	−1.69101	−1.59813	−1.75031	−2.42233	−7.25777
0.20	−5.74679	−2.84415	−1.95515	−1.59484	−1.49334	−1.62845	−2.25645	−6.80552
0.25	−5.65973	−2.75562	−1.86383	−1.49867	−1.38856	−1.50660	−2.09056	−6.35328
0.30	−5.57267	−2.66709	−1.77251	−1.40250	−1.28377	−1.38475	−1.92468	−5.90103
0.35	−5.48561	−2.57857	−1.68119	−1.30633	−1.17899	−1.26289	−1.75879	−5.44878
0.40	−5.39855	−2.49004	−1.58987	−1.21016	−1.07421	−1.14104	−1.59290	−4.99653
0.45	−5.31149	−2.40151	−1.49855	−1.11399	−0.96942	−1.01918	−1.42702	−4.54429
0.50	−5.22443	−2.31299	−1.40723	−1.01782	−0.86464	−0.89733	−1.26113	−4.09204
0.55	−5.13737	−2.22446	−1.31591	−0.92165	−0.75985	−0.77548	−1.09524	−3.63979
0.60	−5.05031	−2.13593	−1.22460	−0.82548	−0.65507	−0.65362	−0.92936	−3.18754
0.65	−4.96325	−2.04741	−1.13328	−0.72931	−0.55029	−0.53177	−0.76347	−2.73530
0.70	−4.87619	−1.95888	−1.04196	−0.63314	−0.44550	−0.40992	−0.59759	−2.28305
0.75	−4.78913	−1.87036	−0.95064	−0.53697	−0.34072	−0.28806	−0.43170	−1.83080
0.80	−4.70207	−1.78183	−0.85932	−0.44080	−0.23593	−0.16621	−0.26581	−1.37855
0.85	−4.61500	−1.69330	−0.76800	−0.34463	−0.13115	−0.04436	−0.09993	−0.92631
0.90	−4.52794	−1.60478	−0.67668	−0.24846	−0.02637	0.07750	0.06596	−0.47406
0.95	−4.44088	−1.51625	−0.58536	−0.15230	0.07842	0.19935	0.23184	−0.02181
1.00	−4.35382	−1.42772	−0.49404	−0.05613	0.18320	0.32121	0.39773	0.43043

TABLE 3. Calculation of vorticity W as a function of ϕ for $\epsilon = 1.00$

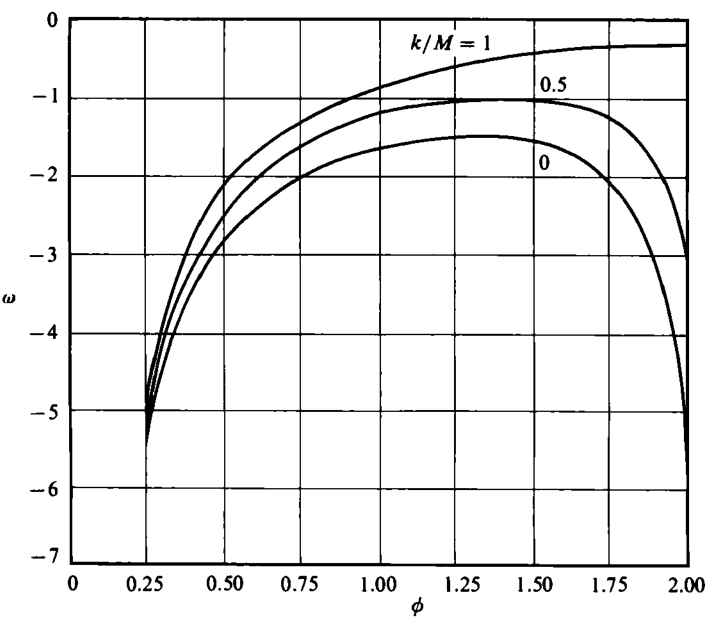

FIGURE 4. Variation of boundary vorticity with angular position for $\epsilon = 0.5$.

change in sign of the vorticity (that is, the vorticity becomes positive in the range $0 < \phi < \frac{2}{3}\pi$). This in turn implies that separation takes place on the boundary when $\epsilon = 0.95$ and $\epsilon = 1$ and the flow rate through the two branches are unequal. In fact separation occurs when most of the flow passes through one branch of the channel. A sketch of the streamlines when separation occurs is given in figure 7.

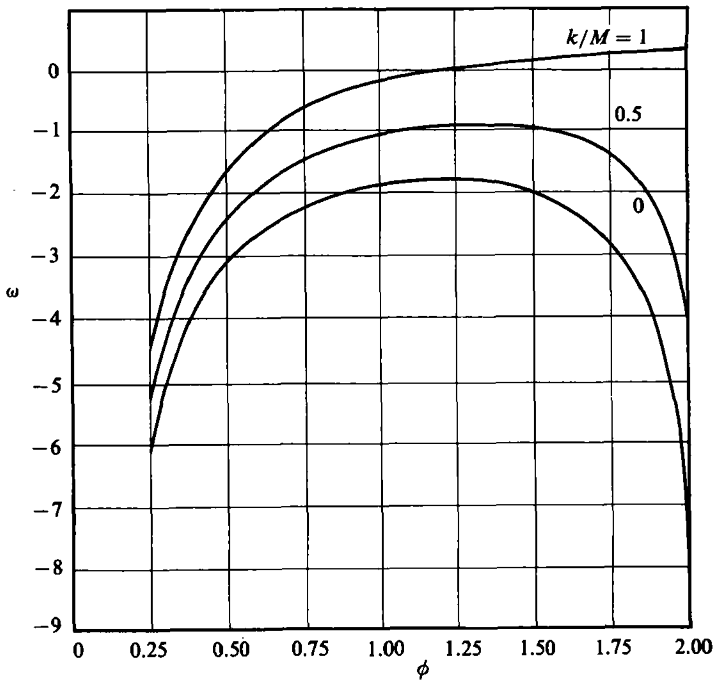

FIGURE 5. Variation of boundary vorticity with angular position for $\epsilon = 0.95$.

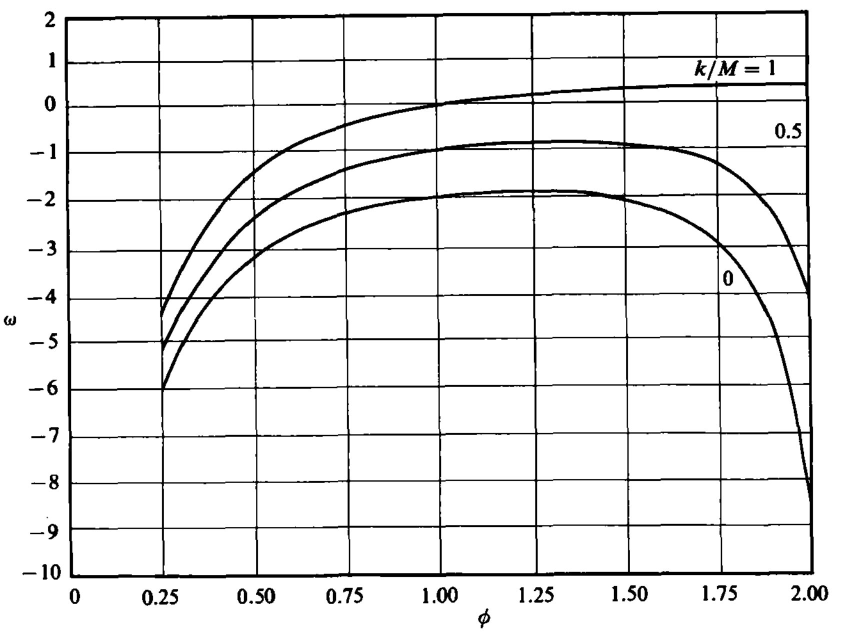

FIGURE 6. Variation of boundary vorticity with angular position for $\epsilon = 1$.

It is of interest to consider values of α in the range $\frac{2}{3}\pi < \alpha < \pi$; that is, when the line sinks move closer to the flow divider. For $\alpha = \frac{3}{4}\pi, \frac{5}{6}\pi$ there is no separation for any value of k/M when $\epsilon = 0.5$ and there is no flow divider. For $\epsilon = 0.95$, there is separation for $\alpha = \frac{3}{4}\pi$ when $k/M = 0.85$, and for $\alpha = \frac{5}{6}\pi$ when $k/M = 0.70$. For the sharp flow divider $\epsilon = 1$ there is separation at $\alpha = \frac{3}{4}\pi$ when $k/M = 0.70$, and at $\alpha = \frac{5}{6}\pi$ when $k/M = 0.55$.

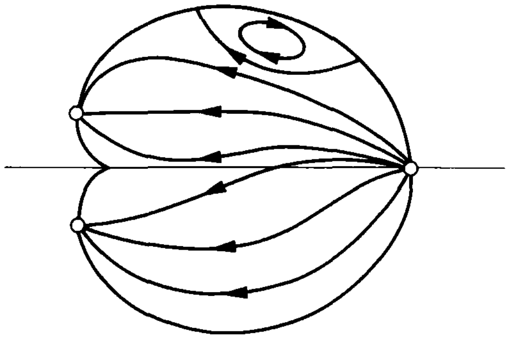

FIGURE 7. Sketch of the streamlines for a smooth flow divider, $\epsilon = 0.95$.

4. The motion in the absence of a flow divider

It is readily shown from Ranger (1961) that the boundary vorticity on the circle $r = 1$, for flow inside it due to a line source of strength $m_1 + m_2$ at $r = 1$, $\theta = \alpha$ and two line sinks of strengths m_1 at $r = 1$, $\theta = -\alpha$ and m_2 at $r = 1$, $\theta = \alpha - 2\beta$, can be expressed by

$$W = 2k_0\{(m_1 + m_2)\cot\tfrac{1}{2}(\theta - \alpha) - m_1\cot\tfrac{1}{2}(\theta + \alpha) - m_2\cot\tfrac{1}{2}(\theta - \alpha + 2\beta)\}, \quad (28)$$

where $0 < \alpha < \pi$, $0 < \beta < \pi$, and k_0 is a constant. It can be verified from (28) that W does not pass through zero and change sign on the circle $r = 1$. This is also the case in §3 for $\epsilon = 0.5$ where the flow divider is absent. Hence the separation that takes place for $\epsilon = 0.95$ and $\epsilon = 1$ can be attributed to the presence of the flow divider, which projects into the fluid region.

5. The special case $\alpha = \frac{2}{3}\pi$, $\epsilon = 1$, $M = k$

In this case the line sink at $\phi = \alpha = \frac{2}{3}\pi$ is absent and the flow is entirely absorbed away by the line sink at $\phi = -\alpha = -\frac{2}{3}\pi$ in the lower half-plane. Equation (27) then simplifies considerably to the following form:

$$\begin{aligned} W = {} & \frac{M}{2\pi}\left\{\frac{5(\sin 3\phi + \sin 2\phi) - 4(\sin 4\phi + \sin 3\phi)}{2(1 - \cos\phi)}\right\} \\ & + \frac{M}{2\pi}\left\{\frac{4[\sin(4\phi + \frac{2}{3}\pi) + \sin 4\phi + \sin(3\phi + \frac{2}{3}\pi) + \sin 3\phi]}{1 - \cos(\phi + \frac{2}{3}\pi)}\right\} \\ & - \frac{M}{2\pi}\left\{\frac{5[\sin 3\phi + \sin(3\phi + \frac{4}{3}\pi) + \sin 2\phi + \sin(2\phi + \frac{4}{3}\pi)]}{1 - \cos(\phi + \frac{2}{3}\pi)}\right\} \\ & - \frac{9M}{2\pi}(\sin\phi + \sin 2\phi) + \frac{M\sqrt{3}}{\pi}(1 + \cos\phi). \end{aligned} \quad (29)$$

Some numerical values for the boundary vorticity are listed in tables 1–3, indicating separation in the upper half-plane. In fact, for the situation $k = M$, $\epsilon = 1$, where there is no sink in the upper half-plane, the separation region extends right up to the cusp.

In conclusion, the numerical values indicate that when the sink is sufficiently strong in the lower half-plane then separation takes place in the upper half-plane. These results are consistent with the experimental results for two- and three-dimensional flows in bifurcating channels. The separation will also be present in a three-dimensional model with a plane of symmetry. The separation will take place in the plane of symmetry, but elsewhere will be modified by the effects of azimuthal swirl.

As the Reynolds number increases from zero the flow is likely to be more concentrated in the region of streamlines joining the source and sink of stronger strength, as it is in the situation of Jeffery–Hamel flow. The region of stagnant fluid in the upper half-plane will become significant in producing reversed flow as the Reynolds number is increased. Batchelor (1967) has sketched the streamlines for uniform flow through a pipe towards a sudden enlargement. This suggests that the eddy region will be larger and the point of attachment (and reattachment) for the bounding streamline will occur closer to source and the sink of weaker strength respectively.

Appendix A

The difference equation (18) can be written as

$$(-\epsilon)^{n+1} B_{n+1} - (-\epsilon)^{n+2} B_{n+2} = (-1)^n \epsilon^n \frac{M}{\pi}(1-\cos n\alpha) \qquad \text{(A 1)}$$

for $n \geqslant 3$. Summing from $n = 3$ to $n = m$ gives

$$\epsilon^4 B_4 - (-1)^{m+2} \epsilon^{m+2} B_{m+2} = \sum_{n=3}^{m} (-1)^n \epsilon^n \frac{M}{\pi}(1-\cos n\alpha) \qquad \text{(A 2)}$$

$$= \frac{M}{\pi} \sum_{n=1}^{m} (-\epsilon)^n (1-\cos n\alpha) + \frac{M\epsilon}{\pi}(1-\cos\alpha) - \frac{M}{\pi}\epsilon^2(1-\cos 2\alpha). \qquad \text{(A 3)}$$

Employing the result

$$\sum_{n=1}^{m} (-\epsilon)^n \cos n\alpha = -\frac{-\epsilon\cos\alpha - \epsilon^2 + (-1)^m \epsilon^{m+1}\cos(m+1)\alpha + (-1)^m \epsilon^{m+2}\cos m\alpha}{1+2\epsilon\cos\alpha+\epsilon^2}, \qquad \text{(A 4)}$$

it follows that for $m \geqslant 3$

$$(-1)^m \epsilon^{m+2} B_{m+2} = \epsilon^4 B_4 + \frac{M\epsilon^2}{\pi}(1-\cos 2\alpha) - \frac{M\epsilon}{\pi}(1-\cos\alpha) + \frac{M\epsilon}{\pi}\frac{1-(-\epsilon)^m}{1+\epsilon} + \frac{M}{\pi}\left\{-\frac{\epsilon\cos\alpha - \epsilon^2 + (-1)^m\epsilon^{m+1}\cos(m+1)\alpha + (-1)^m\epsilon^{m+2}\cos m\alpha}{1+2\epsilon\cos\alpha+\epsilon^2}\right\}. \qquad \text{(A 5)}$$

In order to avoid a singularity in the fluid region at $\rho = \epsilon$, $\phi = \pi$ it is necessary to set

$$B_4\epsilon^4 + \frac{M\epsilon^2}{\pi}(1-\cos 2\alpha) - \frac{M\epsilon}{\pi}(1-\cos\alpha) + \frac{M\epsilon}{\pi(1+\epsilon)} - \frac{M(\epsilon\cos\alpha+\epsilon^2)}{\pi(1+2\epsilon\cos\alpha+\epsilon^2)} = 0, \qquad \text{(A 6)}$$

so that for $n \geqslant 3$

$$B_{n+2} = -\frac{M}{\pi\epsilon}\frac{1}{1+\epsilon} + \frac{M}{\pi\epsilon}\frac{\cos(n+1)\alpha}{1+2\epsilon\cos\alpha+\epsilon^2} + \frac{M}{\pi}\frac{\cos n\alpha}{1+2\epsilon\cos\alpha+\phi^2}. \qquad \text{(A 7)}$$

The boundary conditions for the Fourier components $\sin\phi$ and $\sin 2\phi$ yield

$$2\epsilon B_2 + 2\epsilon^2 B_3 - \epsilon^2 B_1 = \frac{2M}{\pi}(\cos\alpha - 1). \qquad \text{(A 8)}$$

$$\epsilon B_3 + \epsilon^2 B_4 = \frac{M}{\pi}(\cos 2\alpha - 1). \qquad \text{(A 9)}$$

Without loss of generality, $B_1 = 0$, and the series

$$\sum_{n=2}^{\infty} B_n \rho^n \sin n\phi = B_2\rho^2 \sin 2\phi + B_3\rho^3 \sin 3\phi + B_4\rho^4 \sin 4\phi - \frac{M}{\pi\epsilon(1+\epsilon)} \sum_{n=3}^{\infty} \rho^{n+2} \sin (n+2)\phi + \frac{M}{\pi\epsilon} \sum_{n=2}^{\infty} \frac{\rho^{n+2} \sin (n+2)\phi \cos (n+1)\alpha}{1+2\epsilon \cos\alpha + \epsilon^2} + \frac{M}{\pi} \sum_{n=2}^{\infty} \frac{\rho^{n+2} \sin (n+2)\phi \cos n\alpha}{1+2\epsilon \cos\alpha+\epsilon^2}. \tag{A 10}$$

The three series in (A 10) can be summed by standard methods for $0 \leqslant \rho < 1$, and

$$\begin{aligned} \sum_{n=2}^{\infty} B_n \rho^n \sin n\phi &= B_2\rho^2 \sin 2\phi + B_3\rho^3 \sin 3\phi + B_4\rho^4 \sin 4\phi - \frac{M}{\pi\epsilon(1+\epsilon)} \frac{\rho^5 \sin 5\phi - \rho^6 \sin 4\phi}{1-2\rho\cos\phi+\rho^2} \\ &+ \frac{M}{2\pi\epsilon}\left\{\frac{\rho^5 \sin (5\phi+4\alpha) - \rho^6 \sin (4\phi+3\alpha) + \epsilon\rho^5 \sin(5\phi+3\alpha) - \epsilon\rho^6 \sin(4\phi+2\alpha)}{(1+2\epsilon\cos\alpha+\epsilon^2)(1-2\rho\cos(\phi+\alpha)+\rho^2)}\right\} \\ &+ \frac{M}{2\pi\epsilon}\left\{\frac{\rho^5 \sin (5\phi-4\alpha) - \rho^6 \sin (4\phi-3\alpha) + \epsilon\rho^5 \sin(5\phi-3\alpha) - \epsilon\rho^6 \sin(4\phi-2\alpha)}{(1+2\epsilon\cos\alpha+\epsilon^2)(1-2\rho\cos(\phi-\alpha)+\rho^2)}\right\}. \end{aligned} \tag{A 11}$$

Appendix B

The difference equation for D_n in (23) can be written in the form

$$(-\epsilon)^{n+1} D_{n+1} - (-\epsilon)^{n+2} D_{n+2} = \frac{k}{\pi}(-1)^{n+1} \epsilon^n \sin n\alpha. \tag{B 1}$$

If (B 1) is summed from $n = 3$ to $n = m$ then

$$D_4\epsilon^4 + \epsilon(-\epsilon)^{m+1} D_{m+2} = -\frac{k}{\pi} \sum_{n=3}^{m} (-\epsilon)^n \sin n\alpha \tag{B 2}$$

$$= -\frac{k}{\pi} \sum_{n=1}^{m} (-\epsilon)^n \sin n\alpha - \frac{k\epsilon}{\pi} \sin\alpha + \frac{k\epsilon^2}{\pi} \sin 2\alpha. \tag{B 3}$$

Now utilizing the result

$$\sum_{n=1}^{m} (-\epsilon)^n \sin n\alpha = \frac{\{-\epsilon \sin\alpha + \epsilon^{m+1}(-1)^m \sin(m+1)\alpha + (-1)^m \epsilon^{m+2} \sin m\alpha\}}{1+2\epsilon\cos\alpha+\epsilon^2}, \tag{B 4}$$

it follows that for $n \geqslant 3$

$$(-1)^{n+1}\epsilon^{n+2} D_{n+2} = \frac{k\epsilon \sin\alpha - k\epsilon^{n+1}(-1)^n \sin(n+1)\alpha - k(-1)^n \epsilon^{n+2} \sin n\alpha}{\pi(1+2\epsilon\cos\alpha+\epsilon^2)} - \frac{k\epsilon}{\pi}\sin\alpha + \frac{k\epsilon^2}{\pi}\sin 2\alpha - D_4\epsilon^4. \tag{B 5}$$

In order to eliminate a singularity in the fluid-velocity field at $\rho = \epsilon$, $\phi = \pi$ it is necessary to choose

$$D_4 \epsilon^4 = \frac{k}{\pi}\epsilon^2 \sin 2\alpha - \frac{k\epsilon}{\pi}\sin\alpha + \frac{k\epsilon \sin\alpha}{\pi(1+2\epsilon\cos\alpha+\epsilon^2)}, \tag{B 6}$$

so that

$$D_{n+2} = \frac{k\sin(n+1)\,\alpha + k\epsilon\sin n\alpha}{\pi\epsilon(1+2\epsilon\cos\alpha+\epsilon^2)}, \quad n \geqslant 3. \tag{B 7a}$$

The Fourier coefficients for $n = 0, 1, 2$ yield

$$\epsilon D_1 + \epsilon^2 D_2 = 0, \tag{B 7b}$$

$$2\epsilon D_2 + \epsilon^2 D_1 + 2\epsilon^2 D_3 = \frac{2k}{\pi}\sin\alpha, \tag{B 8}$$

$$\epsilon D_3 + \epsilon^2 D_4 = \frac{k\sin 2\alpha}{\pi}. \tag{B 9}$$

Without loss of generality, the coefficient $D_0 = 0$, and the series

$$\sum_{n=3}^{\infty} D_{n+2}\rho^{n+2}\cos(n+2)\,\phi = \frac{k}{\epsilon\pi}\sum_{n=3}^{\infty}\rho^{n+2}\frac{(\sin(n+1)\,\alpha+\epsilon\sin n\alpha)\cos(n+2)\,\phi}{1+2\epsilon\cos\alpha+\epsilon^2}. \tag{B 10}$$

The series in (B 10) is readily summed for $\rho < 1$, and

$$\begin{aligned}\sum_{n=3}^{\infty} D_{n+2}\rho^{n+2}\cos(n+2)\,\phi &= \frac{k\rho^5}{2\pi\epsilon}\left\{\frac{\sin(5\phi+4\alpha)-\rho\sin(4\phi+3\alpha)+\epsilon\sin(5\phi+3\alpha)-\epsilon\rho\sin(4\phi+2\alpha)}{(1+2\epsilon\cos\alpha+\epsilon^2)\,[1+\rho^2-2\rho\cos(\phi+\alpha)]}\right\}\\ &\quad -\frac{k\rho^5}{2\pi\epsilon}\left\{\frac{\sin(5\phi-4\alpha)-\rho\sin(4\phi-3\alpha)+\epsilon\sin(5\phi-3\alpha)-\epsilon\rho\sin(4\phi-2\alpha)}{(1+2\epsilon\cos\alpha+\epsilon^2)\,[1+\rho^2-2\rho\cos(\phi-\alpha)]}\right\}.\end{aligned} \tag{B 11}$$

REFERENCES

BATCHELOR, G. K. 1967 *An Introduction to Fluid Dynamics*, p. 374. Cambridge University Press.

DORREPAAL, J. M. 1979 Stokes flow past a cylindrical lens. *Z. angew. Math. Phys.* **30**, 405–415.

DORREPAAL, J. M., O'NEILL, M. E. & RANGER, K. B. 1976 Axisymmetric Stokes flow past a spherical cap. *J. Fluid Mech.* **75**, 273–286.

PEDLEY, T. J. 1980 *The Fluid Mechanics of Large Blood Vessels*, chap. 5, pp. 235–291. Cambridge University Press.

RANGER, K. B. 1961 A problem on the slow motion of a viscous fluid between two fixed cylinders. *Q. J. Mech. Appl. Maths* **14**, 411–421.

SCHROTER, R. C. & SUDLOW, M. F. 1969 The flow patterns in models of the human bronchial airways. *Respir. Physiol.* **7**, 341–355.

SMITH, K. A., COLTON, C. K. & FREEDMAN, R. W. 1974 Shear stress measurements at bifurcations. In *Proc. Conf. Fluid Dynamic Aspects of Arterial Disease, Columbus, Ohio, 19–20 September, 1974*, pp. 12–15.